applied sciences

MDPI

Article

Magnetic Levitation Actuation and Motion Control System with Active Levitation Mode Based on Force Imbalance

Guancheng Liu [1], Yonghua Lu [1,*], Jiajun Xu [1], Zhanxiang Cui [1] and Haibo Yang [2]

[1] College of Mechanical and Electrical Engineering, Nanjing University of Aeronautics and Astronautics, Nanjing 210016, China
[2] School of Mechanical Engineering, Nanjing Vocational University of Industry Technology, Nanjing 210023, China
* Correspondence: nuaa_lyh@nuaa.edu.cn

Abstract: Accurate large-displacement magnetic levitation actuation and its stability remain difficult in non-liquid environments. A magnetic levitation actuation and motion control system with active levitation mode is proposed in this paper. The actuating force of the system is generated by the external magnetic field. A neural network proportion-integration-differentiation (PID) controller is designed for active actuation, and a force imbalance principle is built for the step motion mode. Dual electromagnetic actuators are configured to generate a superimposed magnetic field, ensuring that the electromagnetic force on the ball is more uniform and stable than single actuators. Dual-hall-structure sensors are used to measure displacement, thereby reducing overshoot and ensuring stability whilst motivating the ball. Due to the high adaptability of the neural network to complex systems with nonlinear and ambiguous models, the PID controller composed of neurons has stronger adaptability through tuning the PID controller parameters automatically. Furthermore, the proposed controller can solve the shortcoming that the deviation between the controlled object and the steady-state operating point increases and the tracking performance deteriorates rapidly. The strong robustness and stability in active levitation and motion control is achieved during both ascending and descending processes.

Keywords: electromagnetic field; active levitation; magnetic levitation actuation; motion control; force imbalance

check for updates

Citation: Liu, G.; Lu, Y.; Xu, J.; Cui, Z.; Yang, H. Magnetic Levitation Actuation and Motion Control System with Active Levitation Mode Based on Force Imbalance. *Appl. Sci.* **2023**, *13*, 740. https://doi.org/10.3390/app13020740

Academic Editor: Emanuele Carpanzano

Received: 25 October 2022
Revised: 25 December 2022
Accepted: 29 December 2022
Published: 4 January 2023

Copyright: © 2023 by the authors. Licensee MDPI, Basel, Switzerland. This article is an open access article distributed under the terms and conditions of the Creative Commons Attribution (CC BY) license (https://creativecommons.org/licenses/by/4.0/).

1. Introduction

A magnetic levitation system is a system that uses magnetic force to overcome gravity to levitate objects. This system makes objects free from their own gravity. Magnetic levitation actuation is a technology that uses a magnetic levitation system to keep the object in and maintain a stable levitation state, and drives the controlled object to perform specific movements in a non-contact manner. The applications of traditional magnetic levitation actuation methods are basically in a liquid environment, and the controlled object is floated on the surface of the liquid or levitated in the liquid by the buoyancy of the liquid when actuated [1–7]. The methods in liquid adopt passive levitation, which has great limits in an application environment. These methods are only suitable for a small area near the working point and cannot deal with relatively large-scale position control. Donghak Byun [8] of the Department of Mechanical Engineering at Chonnam National University in South Korea developed a tadpole-type swimming micro-robot. The micro-robot is actuated by an alternating magnetic field composed of two pairs of vertical Helmholtz coils, and the form of motion is tail swing. The direction and frequency of the tail swing are adjusted by magnetic field changes. Seungmun Jeon [9] of Hanyang University in South Korea proposed a method that uses a combination of a gradient magnetic field and a uniform magnetic field to actuate a spiral micro-robot. This method provides a new navigation and drilling method for dredging blood vessel blockages. Ye Bo [10] proposed a magnetic spiral Wireless Capsule Endoscope (WCE) method based on rotating permanent magnets,

in which the distance between the external permanent magnet and the magnetic spiral WCE is controlled to basically cancel the gravity and magnetic attraction of the magnetic spiral WCE. Under this condition, the WCE is levitated during the motion.

In the industrial and medical fields, most of the magnetic levitating motion requires precise and larger displacement of active motion control. However, there is no dynamic model for the actuating force generated by the rotating magnetic field in current studies, and the control implementation is insufficient [11,12]. Relying on the special structure of the controlled object under the action of an external magnetic field, the object rotates in the liquid to generate a propulsive force, thereby realizing the levitating motion of the controlled object [13,14]. Liquid is a considerable limitation. Without liquid, there is no active levitation ability. As a result, the levitating motion obtained by liquid cannot be applied in a non-liquid environment, and the application range of magnetic levitation actuation technology is relatively limited. The only simple and single levitating motion of the controlled object in liquids can be performed using current methods, and the feedback control and programmable trajectory control cannot be achieved. Consequently, the application of the current method is limited. Importantly, the actual operation of the magnetic levitation actuation is mostly applied in the air environment. Active magnetic levitation actuation technology has promising application prospects in practical industrial and medical fields.

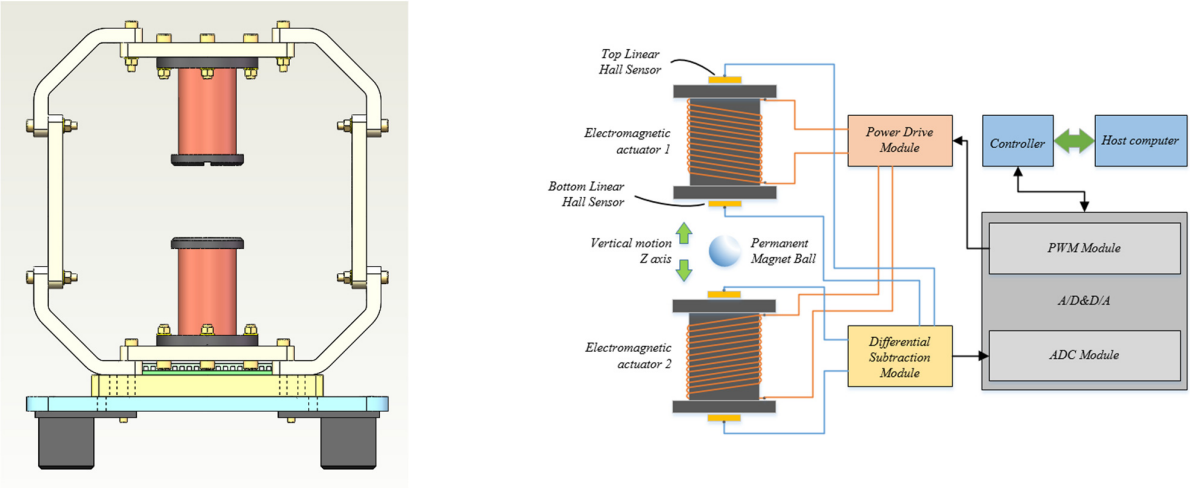
For active magnetic levitation actuation technology, Hamal Marino [15] of the University of Pisa proposed an active magnetic levitation method to achieve controlled helical motion of microrobots in viscous liquid. Maglev ball systems have been extensively studied as applications for active levitation control. Jinggang Zhang [16] use an integral state feedback control method based on a fuzzy model to realize stable position control of the ball. However, most previous studies have only performed short-distance equilibrium position changes to verify the stability of the levitation [16–18]. In the previous research the model-based controller was used, which can achieve the levitating motion control of the permanent magnet ball within a certain range and under a specific step length. However, during the motion process, the fixed Proportion Integration Differentiation (PID) parameters cannot effectively adjust the large position mutation, resulting in excessive overshoot, which causes the controlled ball to vibrate during the step motion. There is severe jittering and even "falling out of control" when using larger step sizes for motion control. Even when using a large step size for motion control there is a violent jitter, and also an uncontrolled fall. There is high adaptability of the neural network to complex systems with nonlinear and ambiguous models. In order to improve the stability of the motion process, the PID controller composed of neurons has stronger adaptability.

The contribution of the paper is presented as follows:

1. An active magnetic levitation actuation system is built, and a dynamic model of the actuation system based on force imbalance is established. The relationship between the levitating motion of the electromagnetically actuated object and the external magnetic field is revealed in the model;
2. A controller combining neural network and PID is adopted to control the electromagnetic actuators, in which the PID control parameters are adjusted through a neural network. This controller eliminates the uncertainties of the complex external magnetic field actuation systems and improves the levitating motion tracking performance. Compared with the model-based controller, the combination of neural network algorithm and PID improves the stability of the magnetic levitating motion. The proposed controller is verified in experiments and simulations, and the result proves that the neural network PID control outperforms the model-based controller;
3. The magnetic levitation actuation and motion control system based on force imbalance can realize non-contact stable levitation. Large-displacement levitating motion of the controlled object in non-magnetic slender pipes can be realized by the proposed step-by-step actuation control method, including other detection and operation equipment attached to the sphere. Non-destructive quality inspection and dredging of the inner wall of slender pipes in the industrial fields can be applied by the control system.

2. System Description

The magnetic levitation actuation and motion control system based on force imbalance consists of a main control unit, power supply modules, electromagnetic actuators, input control modules of current, PWM output modules, differential calculation modules of signals and A/D modules of input signals. The schematic diagram of the magnetic levitation actuation and motion control system based on force imbalance is shown in Figure 1. The electromagnetic actuator adopts dual electromagnets with a symmetrical layout to generate a superimposed magnetic field to attract the control component of a permanent magnet ball. The system forms a feedback closed loop through the position signals and current signals collected by sensors, so that the control component can move according to the required path and accuracy, thereby realizing the operation and control of the permanent magnet ball in a non-liquid environment. During the actuating process, the ball can move with variable speeds and controllable trajectory.



(**a**) (**b**)

Figure 1. Mechanical structure and system control model of magnetic levitation system. (**a**) External magnetic field actuation device; (**b**) System control model.

The parameters of electromagnetic actuators 1 and 2 are the same, which are given in Table 1. The permanent magnet ball is made of NdFeB, and B_s = 677.3 mT. In addition, the ball's radius r = 6.35 mm and mass m = 8.15 g.

Table 1. Related parameters of electromagnetic actuators.

Parameter	Description	Value
N	number of coils	1445
R_1	inner radius	7.5 (mm)
R_2	outer radius	20 (mm)
L	winding height	60 (mm)
R	resistance of coil	9.3 (Ω)
d	diameter of copper wire	0.71 (mm)
L_0	overall length of coil	80,743.13 (mm)
S	coil cross-sectional area	678.24 (mm^2)
A	surface area of coil	10,399.68 (mm^2)

It can be seen from Figure 2 that the permanent magnet ball is located on the central axis of the electromagnetic solenoid along the Z direction, and the electromagnetic force generated by the external magnetic field actuates the ball to move in the direction where the magnetic induction intensity changes most rapidly. The force with cylindrical symmetry in the XY plane can be ignored because it has a total effect of zero on the permanent magnet

ball. From $(\partial B_Z)/\partial z$, the electromagnetic force F exerted by the hollow solenoid on the permanent magnet ball [19–21] is:

$$F = (m \bullet \nabla)B = |m|\frac{\Delta B_z}{\Delta z} = \frac{3B_s}{2\mu_0}V_b \bullet \frac{\partial B_z}{\partial z} \quad (1)$$

where F denotes the electromagnetic force on the permanent magnet ball; m denotes the mass of the permanent magnet ball; B denotes magnetic field of electromagnetic actuators; ∇ denotes gradient; B_z denotes magnetic field of electromagnetic actuators in vertical direction; B_s denotes magnetic field of the permanent magnet ball; V_b denotes the volume of the permanent magnet ball; μ_0 denotes vacuum permeability.

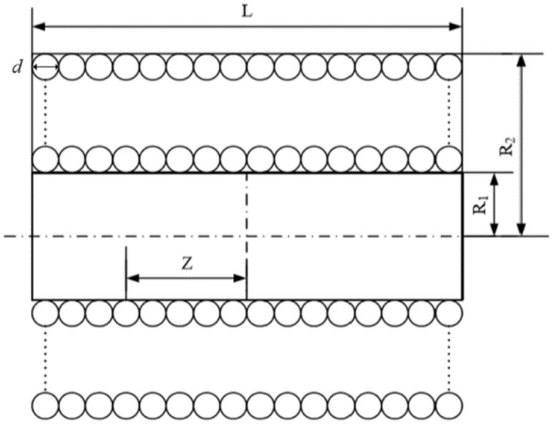


Figure 2. Schematic diagram of multilayer solenoid structure.

F on the permanent magnet ball is correlated to the current i and the levitation gap δ of the permanent magnet ball, and F is proportional to the magnitude of current i through the coil from (1). Moreover, the electromagnetic force exerted by the dual electromagnetic actuators on the permanent magnet ball is a superposition of both electromagnetic forces. The dimensionless equation of F is simplified from (1) based on the external magnetic field actuation, and then the electromagnetic force F exerted by the dual electromagnetic actuators on the permanent magnet ball is superimposed in the Z axis direction to obtain the following equation.

$$F(\delta_1, \delta_2, i_1, i_2) = \frac{d_1 i_1}{a_1(\delta_1 - r)^2 + b_1(\delta_1 - r) + c_1} - \frac{d_2 i_2}{a_2(\delta_2 - r)^2 + b_2(\delta_2 - r) + c_2} \quad (2)$$

where F (δ_1, δ_2, i_1, i_2) (N) denotes the electromagnetic force on the permanent magnet ball; X (m) denotes the gap between the electromagnetic actuator 1 and the electromagnetic actuator 2; i_1 and i_2 (A) are, respectively, the excitation currents of the coil windings of the electromagnetic actuator 1 and the electromagnetic actuator 2; δ_1 and δ_2 (m) denote the levitation gap from the center of the permanent magnet ball to the hall sensors at the lower end of the electromagnetic actuator 1 and at the top of the electromagnetic actuator 2, i.e., $\delta_1 + \delta_2 = X$. The parameters a_1, a_2, b_1, b_2, c_1, c_2, d_1 and d_2 in the (2) are the coefficients determined by the force imbalance control system.

Based on (2) and the principles of Newton's Second Law, the dynamic equation of the permanent magnet ball is constructed. Within the reasonable range of levitation gap, the nonlinear model is replaced by the approximate linear model to establish the dynamic model of the permanent magnet ball. According to Figure 3, the dynamic model of the magnetic levitation actuation and motion control system is:

$$\frac{md^2\delta_1}{dt^2} + k_{\delta 1}\delta_1 + k_{i1}i_1 + k_{i2}i_2 = f_d \quad (3)$$

where $k_{\delta 1} = \partial F/\partial_{\delta 1}$, k_δ (N/m) is the displacement stiffness coefficient; $k_{i1} = \partial F/\partial i_1$, k_{i1} (N/A) is the current stiffness coefficient of i_1; $k_{i2} = \partial F/\partial_{i2}$, k_{i2} (N/A) is the current stiffness coefficient of i_2; f_d (N) denotes external interference.

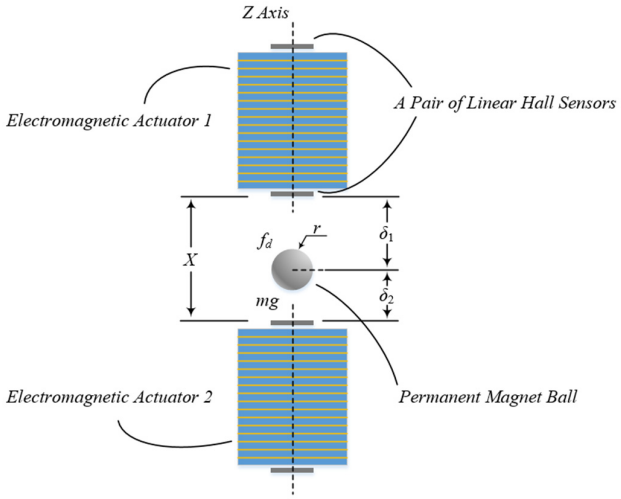


Figure 3. External magnetic actuation model of dual electromagnetic actuators.

3. Control Method

The permanent magnet ball is in equilibrium under the action of dual electromagnets placed vertically. In order to change the displacement of the permanent magnet ball in the vertical position, it is necessary to break the equilibrium of forces acting on the ball. After removing the external magnetic field of the permanent magnet ball and adding the magnetic field instantaneously, the external force and motion of the permanent magnet ball undergo an instantaneous mutation. The process of rebalancing after constant imbalance is called the process of force imbalance. In the process of control, force imbalance is only an instantaneous state of breaking the equilibrium, so it is necessary to accurately control the imbalance and equilibrium of the force. The momentary magnetic imbalance causes the displacement of the permanent magnet ball to change, and the equilibrium is maintained immediately by control. The force control principle that realizes the ball from equilibrium to imbalance and then to equilibrium is called the force imbalance control principle.

Neural network covers comprehensive and diverse fields, including computer vision (including image and video fields), voice fields, text-oriented natural language processing, intelligent actuation, smart cities, medical care, and other aspects of life. It is often used to solve nonlinear systems with uncertainties, which is its area of expertise. Because neural network has good adaptability to complex systems with nonlinear and ambiguous models [22,23], it has been widely used in the field of magnetic levitation technology [24,25].

Neural network has good tracking performance. PID control with neural network algorithm can change the PID parameters in real time according to the position change of the ball during control, so that the magnetic levitation system always maintains good control ability. The permanent magnet ball obtains a better stable levitation state and levitating motion performance within the levitation range. Neural network PID controller is adopted to actuate a new external magnetic field in the paper, which relies on the actuation principles of force imbalance.

For the magnetic levitation actuation and motion control system, the electromagnetic force is exerted by the electromagnetic actuators on the permanent magnet ball. No matter how the position of the permanent magnet ball changes, the upper electromagnetic force always maintains 2 *mg* (twice the gravity of the ball), and the lower electromagnetic force always maintains mg. The dynamic models of the electromagnetic actuators 1 and 2 are established, respectively. Laplace transformations are performed on the model, in which the excitation currents $I_1(s)$ and $I_2(s)$ are used as input, whilst the vector combination of

levitation gaps $[\delta_1\ \delta_2]^{\mathrm{T}}$ is the output. The magnetic levitation actuation and motion control system of the permanent magnet ball are established as:

$$\begin{bmatrix}\delta_1\\ \delta_2\end{bmatrix} = \begin{bmatrix}(-\frac{k_{i1}}{m})/(s^2+\frac{k_{\delta 1}}{m}) & 0\\ 0 & (-\frac{k_{i2}}{m})/(s^2+\frac{k_{\delta 2}}{m})\end{bmatrix}\begin{bmatrix}I_1\\ I_2\end{bmatrix} \tag{4}$$

where k_{i1} and k_{i2} (N/A) are, respectively, the current stiffness coefficients of the upper and lower actuators; $k_{\delta 1}$ and $k_{\delta 2}$ (N/m) are the displacement stiffness coefficients of the upper and lower actuators, respectively; $I_1(s)$ and $I_2(s)$ are the Laplace transform of the coil winding currents of electromagnetic actuators 1 and 2, respectively; $\delta_1(s)$ and $\delta_2(s)$ are the Laplace transform of levitation gaps between the permanent magnet ball and electromagnetic actuators 1 and 2.

Establish the state space model of the actuation system as follows:

$$\begin{aligned}\dot{x} &= \begin{bmatrix}A_{11} & 0\\ 0 & A_{22}\end{bmatrix}x + Bi\\ \delta &= Cx\end{aligned} \tag{5}$$

where A_{11} and A_{22} are 2×2 coefficient matrices; B is a 4×2 coefficient matrix; C is a 2×4 coefficient matrix.

According to the mathematical expression of current stiffness coefficient and displacement stiffness coefficient, as the levitation gap increases, $k_{\delta 1}$ and $k_{\delta 2}$ decrease first and then increase. When $\delta_1 > 7.702$ and $\delta_2 > 7.702$ the values of $k_{\delta 1}$ are always negative. When $\delta_1 > 0$ and $\delta_2 > 0$ the values of k_{i1} and k_{i2} are always positive. Furthermore, the values of $k_\delta - k_i$ is always less than zero within the set levitating range. Due to the size of the ball, both δ_1 and δ_2 are greater than 8 mm. According to the Routh Stability Criterion, for the magnetic levitation actuation and motion control system, which is a natural open-loop unstable system, a first term (differential term) must be added to enable the system to achieve stable control.

According to the control models and stability control requirements of the second-order system, neural network PID control is adopted by the magnetic levitation actuation and motion control system actuated, the principles of which are based on force imbalance control theory. The system control block diagram is shown in Figure 4. The proposed controller is a PID controller with adjustable parameters that are determined by neural network.

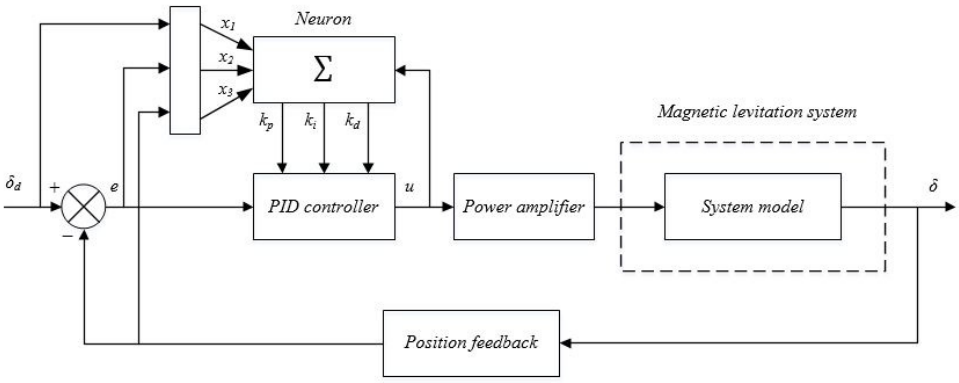


Figure 4. System control block diagram.

The PID controller is formulated as:

$$u(t) = k_p e(t) + k_i \int_0^t e(t)dt + k_d \frac{de(t)}{dt} \tag{6}$$

The derivative is replaced by the backward difference, and the integral is replaced by the sum of the rectangular areas. The state model of the PID controller is:

$$u(k) = k_p e(k) + k_i T \sum_{j=0}^{k} e(j) + k_d [e(k) - e(k-1)] \tag{7}$$

where $e(k) = \delta - \delta_d$, δ is the current position value of ball, δ_d is the desired position value of ball; k denotes the current state; $u(k)$ is the output of neural network PID controller, the physical meaning of which is current $i(k)$ of electromagnetic actuator; $k-1$ denotes the previous state; K_p, K_i and K_d represent the adjustment coefficients of the control system, that is, the proportional, integral, and differential coefficients of the neural network PID controller, respectively; T denotes time constant.

According to the structure of the neural network PID controller, the input equation of controller [26,27] is:

$$\begin{aligned} x_1(k) &= e(k) \\ x_2(k) &= T \sum_{j=0}^{k} e(j) \\ x_3(k) &= [e(k) - e(k-1)]/T \end{aligned} \tag{8}$$

The simplified output equation is:

$$u(k) = w_1(k)x_1(k) + w_2(k)x_2(k) + w_3(k)x_3(k) \tag{9}$$

where $w_i(k)$ denotes the weighting coefficients of the neuron input $x_i(k)$, i.e., the proportional coefficient k_p, integral coefficient k_i and differential coefficient k_d in (7).

These adjustment coefficients are adjusted by the gradient descent algorithm of neuron weight correction, and the adjustment law is:

$$\begin{aligned} w_1(k) &= w_1(k-1) + \eta e(k) x_1(k) \frac{\partial \delta(k+1)}{\partial u(k)} \\ w_2(k) &= w_2(k-1) + \eta e(k) x_2(k) \frac{\partial \delta(k+1)}{\partial u(k)} \\ w_3(k) &= w_3(k-1) + \eta e(k) x_3(k) \frac{\partial \delta(k+1)}{\partial u(k)} \end{aligned} \tag{10}$$

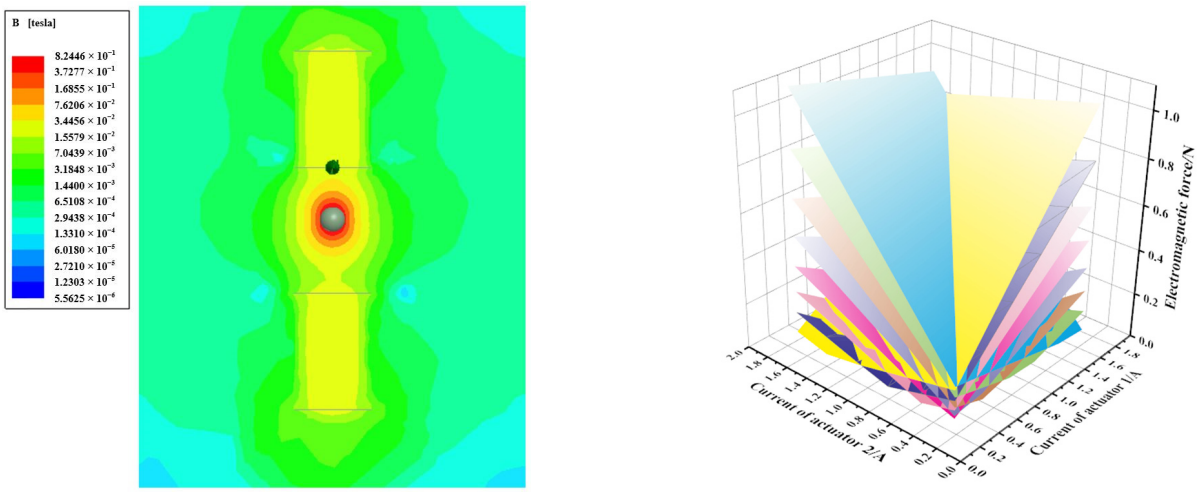
where η denotes the learning rate, and $0 < \eta < 1$; in general, $\partial\delta(k+1)/\partial u(k) \approx (\delta(k+1) - \delta(k))/(u(k) - u(k-1))$ represents an important coefficient that determines the adjustment direction of the weighting coefficient.

4. Force Imbalance Stable Levitation Test

The overshoot $\sigma\%$ is the primary parameter of the active magnetic levitation actuation system. The actual meaning of the overshoot in the paper is the magnitude of position change of the permanent magnet ball in the vertical direction. The overshoot characterizes the feasibility of the permanent magnet ball's levitating motion and the stability during the motion. A lower overshoot can enable the controlled ball to obtain more precise position control in practical applications and reduces the possibility of damage to the inspected surface by the controlled object. Therefore, the optimization of the overshoot is the significance of the active magnetic levitation actuation and the premise of the system stability.

ANSYS Maxwell finite element analysis conditions are closer to the test environment. According to the simulation results of F on the permanent magnet ball, the coefficients a, b, c and d of (2) are fitted by the least square method. The multi-parameter fitting diagram is shown in Figure 5. According to the fitting result, the coefficient values of (2) are $a_1 = a_2 = 111300.000$, $b_1 = b_2 = -301.000$, $c_1 = c_2 = 8.691$, and $d_1 = d_2 = 4.199$. The equation of electromagnetic force F is exerted on the permanent magnet ball by the electromagnetic actuator, i.e.,

$$F(\delta_1, \delta_2, i_1, i_2) = \frac{4.199\, i_1}{111300\,(\delta_1 - r)^2 - 301\,(\delta_1 - r) + 8.69} - \frac{4.199\, i_2}{111300\,(\delta_2 - r)^2 - 301\,(\delta_2 - r) + 8.69} \tag{11}$$



(**a**) (**b**)

Figure 5. External magnetic field simulation and data fitting of the magnetic levitation actuation and motion control system. (**a**) ANSYS Maxell magnetic field simulation of dual electromagnetic actuators; (**b**) Data fitting of electromagnetic force.

Through calculation, the parameter is determined as $k_{i1} = 0.14371$, $k_{\delta 1} = -16.6152$, $k_{i2} = -0.027568$, $k_{\delta 2} = -4.197625$ in (4). According to the actual values of current stiffness coefficients and displacement stiffness coefficients, the coefficient matrices in (5) are:

$$A_{11} = \begin{bmatrix} 0 & 63.69 \\ 32 & 0 \end{bmatrix} A_{22} = \begin{bmatrix} 0 & 16.1 \\ 32 & 0 \end{bmatrix} B = \begin{bmatrix} 1 & 0 \\ 0 & 0 \\ 0 & 0.25 \\ 0 & 0 \end{bmatrix} C = \begin{bmatrix} 0 & -0.551\ 0\ 0 \\ 0\ 0\ 0\ 0.4228 \end{bmatrix} \tag{12}$$

The neural network PID controller and model-based controller are built in the simulation environment, and the simulation results of overshoot and response time are compared. For the simulation conditions the same mathematical model is used, and the same initial parameters are used for different control methods. The parameter values are $k_p = -12.6$, $k_i = -9$ and $k_d = -0.84$. The error variable is used as the discrete input signal of the neural network PID controller system equation, and the output of the system equation is used as the control variable.

For the simulation results of Figure 6, the overshoot of step response output of the neural network PID controller of the magnetic levitation actuation and motion control system is 4.9%, and the overshoot of the model-based controller is 7.5%. Magnetic levitating system with the neuron network PID controller has a better stability. The system with dual actuators has a small overshoot and short adjustment time, so the system has good dynamic and static characteristics. The proposed controller parameters are adjusted more stably, indicating that the mechanical structure of the system is more reasonable, the control method is more applicable, and the tracking error of the control system is smaller. The neural network PID controller with dual electromagnetic actuators can realize the stable levitation of the permanent magnet ball. The steady-state error of output signals is less than 0.1%, which meets system performance requirements.

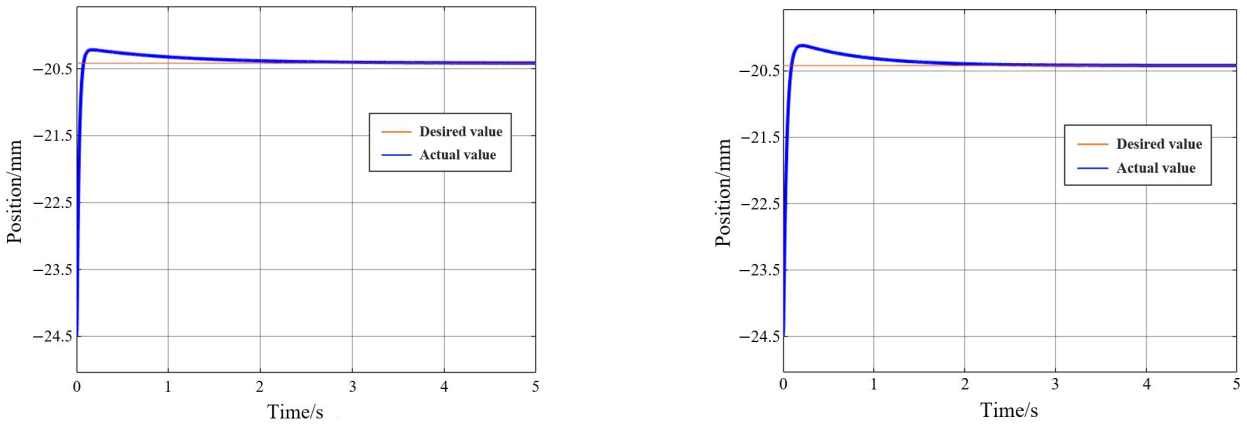


Figure 6. Step response simulation of different controllers with the same electromagnetic actuation structure. (**a**) Step response simulation of neural network PID controller; (**b**) Step response simulation of model-based controller.

In the actual levitation control, the test is carried out in a static and undisturbed air environment, and the ambient temperature is 20 °C. According to the parameters of electromagnetic actuators in Table 1, the maximum heating temperature of the coil is within the working temperature range of the sensor. The skeleton of electromagnetic actuators is made of high-performance nylon with excellent thermal insulation performance.

The position control process is shown in Figure 7. The AH49H type hall sensor is used to collect the position of the permanent magnet ball, and the collection range is ±3000 Gauss. Compared with the laser position sensor and the eddy current sensor, the hall sensor is not affected by the material and light refraction of the detected object and can accurately collect the magnetic field around the permanent magnet ball, making the application scope of active magnetic levitation actuation more extensive. In the process of collecting the magnetic field signal of the permanent magnet ball, the dual-hall sensors are arranged symmetrically in the vertical direction to actively eliminate the influence of the magnetic field of the electromagnetic actuators on the sensors.

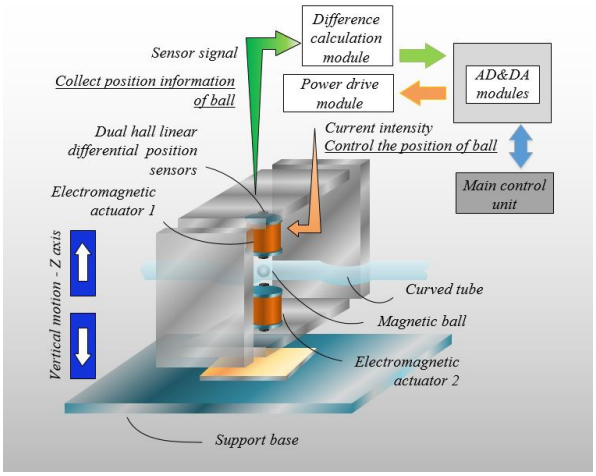


Figure 7. Position control process of the permanent magnet ball.

It is necessary to collect the magnetic field signal of the ball at high frequency to meet the stable levitation of the ball. Too low acquisition frequency will delay the collected magnetic field signal of the ball, resulting in that the control frequency not keeping up with the frequency of the magnetic field change, causing the ball to vibrate violently or even fall.

The software differential has a slow aging time, which affects the control time. Therefore, the OP07 operational amplifiers are used to perform hardware differentials on the voltage signal collected by the dual-hall sensors. The differential result is collected by the 16-bit AD7606, and the data are processed and controlled by the STM32F407 microcontroller. After obtaining the accurate magnetic field signal of the ball, the voltage signal collected by the dual-hall sensors and the actual position of the permanent magnet ball are calibrated. Finally, the corresponding relationship between the position of the permanent magnet ball and the voltage value of the sensors within the levitation range is fitted.

The acquisition accuracy of the AH49H hall sensor is 0.33 mV/Gauss, the calibration accuracy of the test position is 0.002 mm, and the acquisition accuracy of the 16-bit AD7606 is 0.153 mV. The integrated position accuracy of the permanent magnet ball for the test results is 0.002 mm.

The actual levitating control of the magnetic levitation actuation and motion control system is carried out using the designed neural network PID controller, on the premise of the simulation results of the neural network PID control of permanent magnet ball. The control effect of the neural network PID controller on the actual levitating system is studied through experiments. The initial position of the permanent magnet ball is set to −24.50 mm, and the target balance position is set to −20.40 mm. The test results are shown in Figure 8.

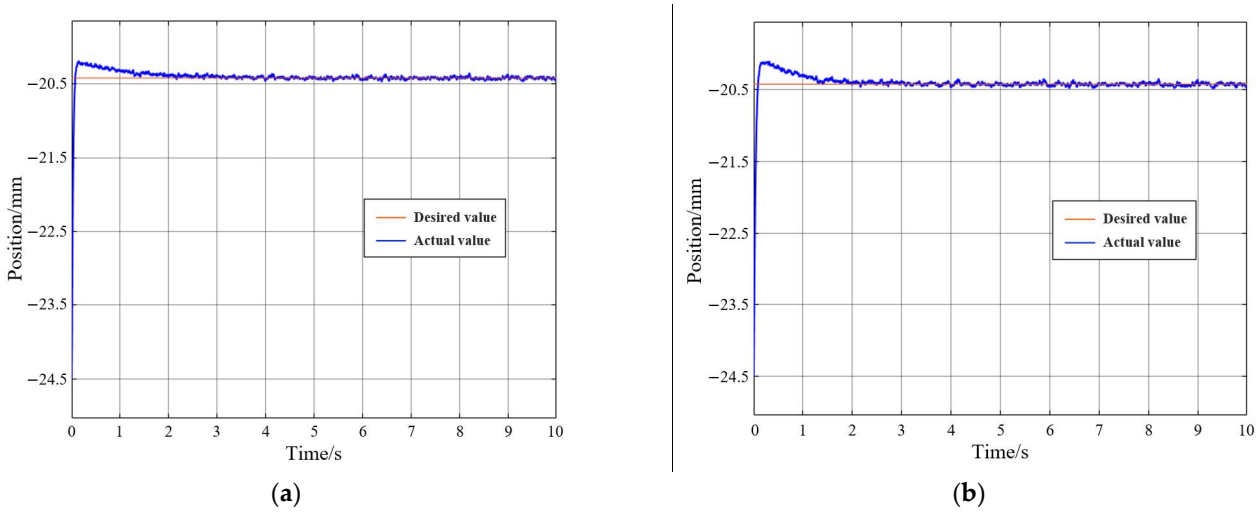


Figure 8. Step response position tracking of the test of different controller with the same electromagnetic actuation structure. (**a**) Neuron network PID controller; (**b**) Model-based controller.

It can be seen from Figure 8 that the permanent magnet ball can achieve stable levitation. The overshoot of the magnetic levitation actuation and motion control system using the neural network PID controller is 5.8%, and the step length is 4.1 mm. The position fluctuation ranges of the permanent magnet ball controlled by the neural network PID controller is 0.31 mm after stable levitation, and the position fluctuation range controlled by the digital PID controller is 0.64 mm after stable levitation. The overshoot using the model-based controller is 7.7%. Comparative test results of the maglev ball system in Literature [18] were collected. The overshoot using sliding mode control is 8.5%, and the overshoot of particle swarm sliding mode-fuzzy PID is 6.7%. The step length of the test results of the two controllers is 2 mm. Compared with these two control systems, the magnetic levitation motion control system proposed in this paper has better system performance by optimizing the actuation structure and control method. By using the neural network PID controller, the magnetic levitation actuation and motion control system has more stable and accurate dynamic and static outputs, better characteristics and stronger anti-interference ability. The neural network PID controller is more suitable for the system.

The test conditions will become inconsistent due to the difference between the simulation model and the actual model. The difference between test results and the simulation results is caused by the shape errors and test condition errors, but the errors are within the allowable range. The actually stable levitation effect of the permanent magnet ball is shown in Figure 9.

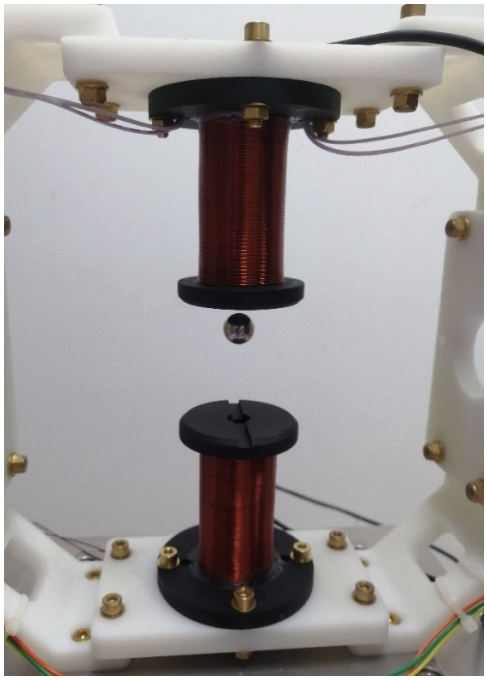


Figure 9. Permanent magnet ball stable levitation effect of the permanent magnet ball.

5. Force Imbalance Levitating Motion Control Test

After achieving the stable levitation, the step-by-step actuation control method is used to realize the long-distance levitating motion control of a permanent magnet ball. Within the control range of the levitation system, the continuous levitating motion is divided into a series of discrete transition points. The position of each discrete point can be derived from the electromagnetic force equation through the system model. Then, the controller parameters of each transition point are obtained through adjustment. For stability of the controlled object, the continuous position of the permanent magnet ball among the transition points is used to realize the actuation, and the control parameters are quickly updated at each step input signal to ensure the levitating stability of the ball at each transition point.

In order to better observe the control effect of the neural network PID controller, the sine signal of $T = 2\pi$ s and square wave signal of $T = 10$ s are used to track and analyze the characteristics of the controller. The simulation results shown in Figure 10 show that the input signal responded well to the control system, and the stable levitation control of the controlled object can be achieved well. The system has a fast response speed and a small tracking error, so it has good dynamic and static performance.

For step-by-step actuation control, when the permanent magnet ball directly responds to a large step input signal, due to the non-linear relationship between electromagnetic force on the permanent magnet ball exerted by the actuators and levitation gap, the ball is prone to drop out of control. In addition, the significant overshoot means that the controlled object's dynamic and static characteristics are not stable and accurate. In order to study the effect of different step inputs on the motion performance, the step inputs are set to 1.0 mm, 0.5 mm and 0.2 mm, respectively. The test results are shown in Figure 11 for the descending motion of the permanent magnet ball from the −19.40 mm to the −20.40 mm and the ascending motion from the −20.40 mm to the −19.40 mm.

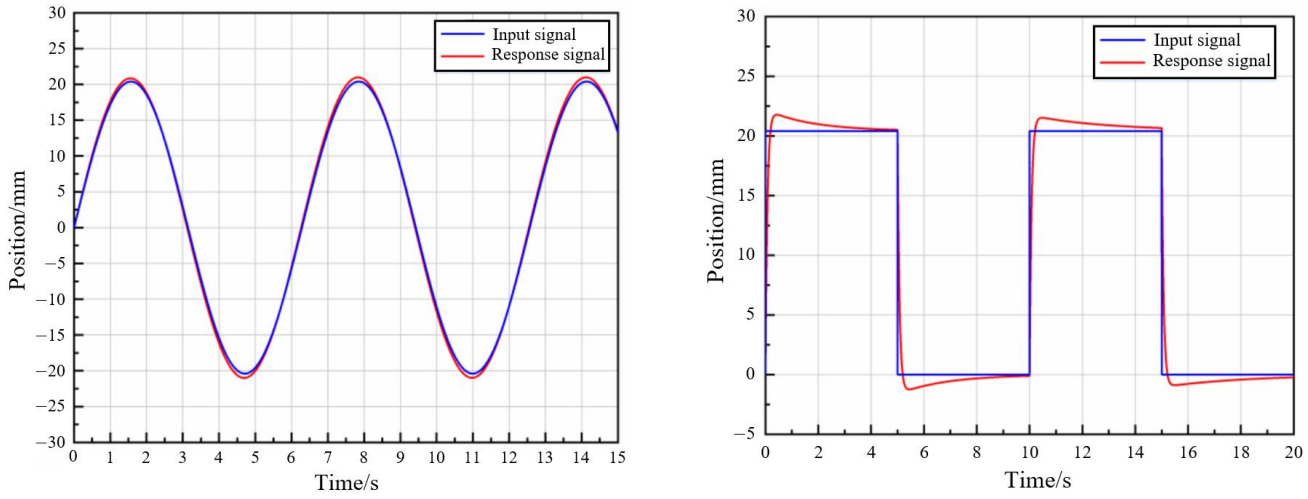


Figure 10. Tracking response of neural network PID control. (**a**) Sine wave tracking simulation; (**b**) Square wave tracking simulation.

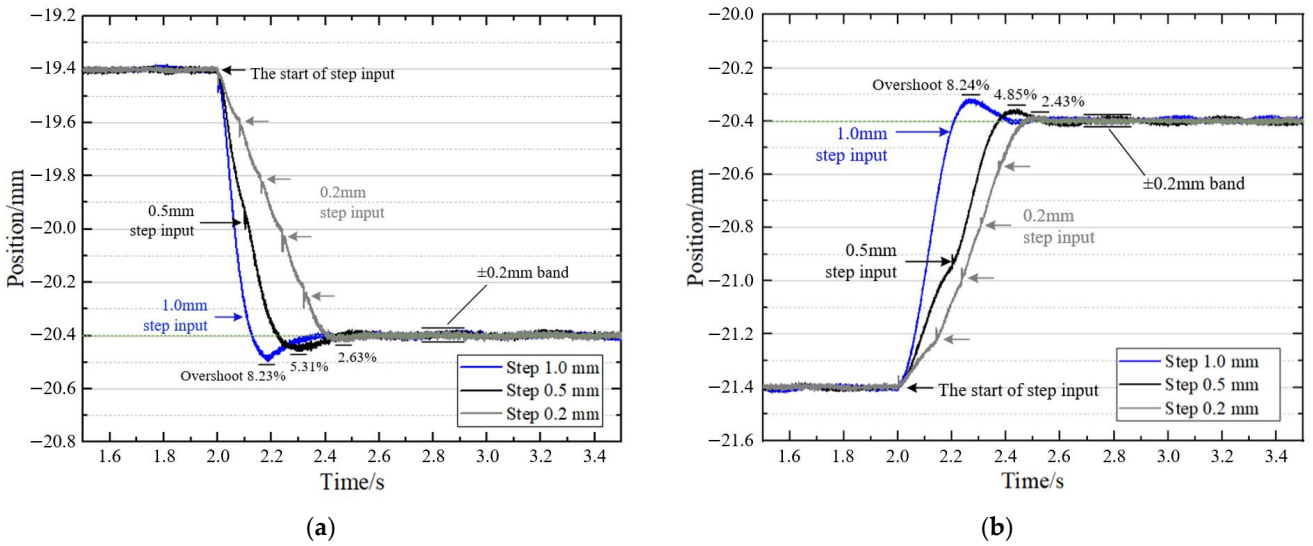


Figure 11. Dynamic real-time position response of three step inputs of controlled levitating object. (**a**) Descending motion; (**b**) Ascending motion.

As can be seen from Figure 11, whether the permanent magnet ball is rising or falling, compared with the direct response, the overshoot of the step response is reduced significantly by using the step-by-step levitating motion control method. The smaller the step is input, the smaller the overshoot becomes. The adjustment time of the step-by-step control is a bit longer than the continuous control, but the step response process is more stable and accurate.

The reliability of test results of different step inputs is verified by 10 sets of repeatability tests. The repeatability test results of the descending motion are shown in Table 2, and the repeatability test results of the ascending motion are shown in Table 3. In Tables 2 and 3, σ% denotes overshoot, t denotes adjustment time, AVG represents average standard, and σ denotes deviation.

Table 2. Comparison of the dynamic characteristics of the repeatability test of descending motion.

No	1.0 mm		0.5 mm		0.2 mm	
	σ%	t/s	σ%	t/s	σ%	t/s
1	8.67%	0.55	5.72%	0.71	2.41%	0.72
2	8.57%	0.52	4.73%	0.69	2.67%	0.81
3	7.57%	0.51	5.03%	0.70	3.14%	0.76
4	7.97%	0.53	5.61%	0.76	2.41%	0.64
5	8.57%	0.58	4.92%	0.72	3.02%	0.75
6	8.07%	0.59	5.72%	0.71	2.40%	0.63
7	7.97%	0.51	5.81%	0.70	2.43%	0.72
8	7.99%	0.48	5.41%	0.68	2.79%	0.76
9	8.48%	0.52	4.76%	0.72	2.41%	0.72
10	8.46%	0.52	5.41%	0.74	2.53%	0.75
AVG	8.23%	0.53	5.31%	0.71	2.63%	0.73
σ	0.35%	0.03	0.40%	0.03	0.26%	0.04

Table 3. Comparison of the dynamic characteristics of the repeatability test of ascending motion.

No	1.0 mm		0.5 mm		0.2 mm	
	σ%	t/s	σ%	t/s	σ%	t/s
1	8.32%	0.66	4.41%	0.84	2.20%	0.81
2	7.93%	0.65	5.32%	0.82	2.76%	0.87
3	8.71%	0.60	5.02%	0.86	2.21%	0.80
4	8.52%	0.68	5.31%	0.72	2.31%	0.84
5	7.63%	0.62	4.61%	0.82	2.65%	0.88
6	8.22%	0.68	4.92%	0.87	2.43%	0.85
7	8.11%	0.64	4.72%	0.82	2.19%	0.84
8	8.72%	0.69	4.52%	0.88	2.54%	0.87
9	8.32%	0.62	4.54%	0.84	2.77%	0.89
10	7.93%	0.61	5.12%	0.80	2.20%	0.82
AVG	8.24%	0.64	4.85%	0.83	2.43%	0.85
σ	0.34%	0.03	0.32%	0.02	0.22%	0.03

It can be seen from Table 3 that during the descending motion, and compared with the 1.0 mm step input, the overshoot of 0.5 mm step input is reduced by 37.3% and the adjustment time is increased by 34.3%. Compared with the 1.0 mm step input, the overshoot of 0.2 mm step length is reduced by 75.4% and the adjustment time is increased by 37.9%. It can be seen from Table 3 that during the ascending motion, and compared to the 1.0 mm step input, the overshoot of 0.5 mm step input is reduced by 42.7% and the adjustment time is increased by 29.7%. Compared to the 1.0 mm step input, the overshoot of 0.2 mm step length is reduced by 74.9% and the adjustment time is increased by 31.1%. The 2 pairs of 10 sets of repeatability test data meet the 3σ criterion.

According to the test data in Tables 2 and 3, plot the change curves of the overshoot and adjustment time of three step inputs in the descending and ascending motion process shown in Figures 12 and 13. The repeatability test results of the descending motion are consistent with the test results shown in Figure 11a, and the repeatability test results of the ascending motion are consistent with the test results shown in Figure 11b. In Figures 12 and 13, l_1 represents overshoot of 1.0 mm step input, l_2 represents overshoot of 0.5 mm step input, l_3 represents overshoot of 0.2 mm step input, l_4 represents adjustment time of 1.0 mm step input, l_5 represents adjustment time of 0.5 mm step input, l_6 represents adjustment time of 0.2 mm step input. Dotted line AVG denotes average value.

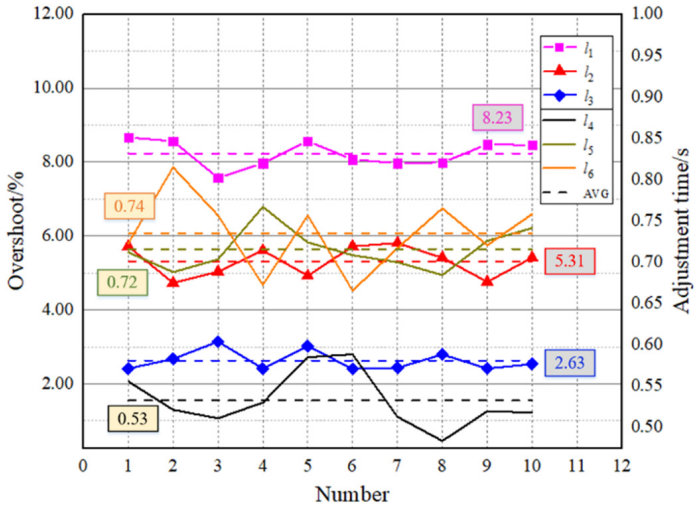


Figure 12. Change curve of overshoot and adjustment time of repeatability test during descending motion.

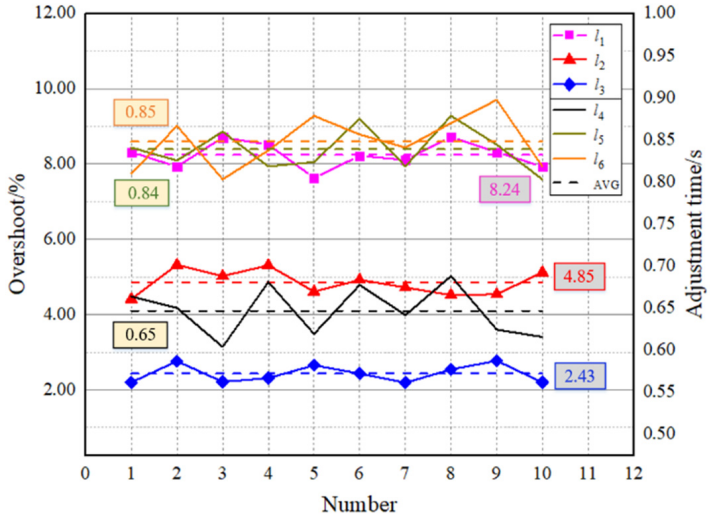


Figure 13. Change curve of overshoot and adjustment time of repeatability test during ascending motion.

When the error band is set to ±0.02 mm for more precise levitation, the adjustment time of the 10 sets of test with a step input of 0.2 mm are greatly affected by the adjustment time evaluation standard, which in turn leads to a certain standard deviation of the adjustment time of the 10 sets of test. The analysis results are applicable to descending and ascending motion.

For a large displacement of stable levitation motion, the effect of the levitating motion during descending motion is shown in Figure 14. The hall sensor near the permanent magnet ball on the electromagnetic actuator #1 is the coordinate origin. The controllable levitation distance of the active magnetic levitation actuation system in the vertical direction is from −34.5 mm to −9.5 mm, and the total levitation range is 25 mm.

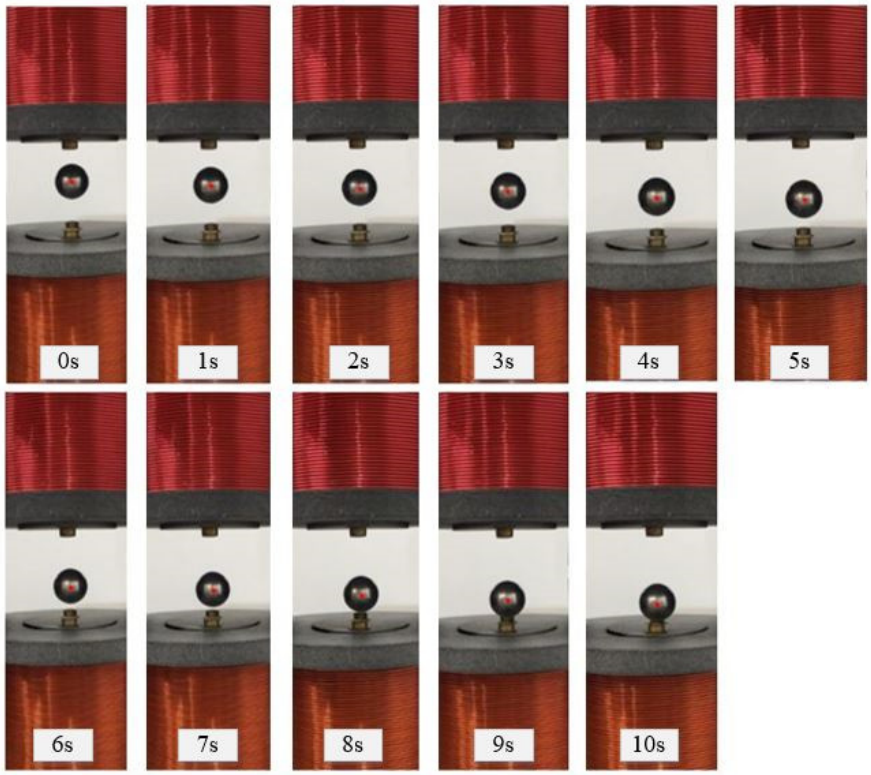
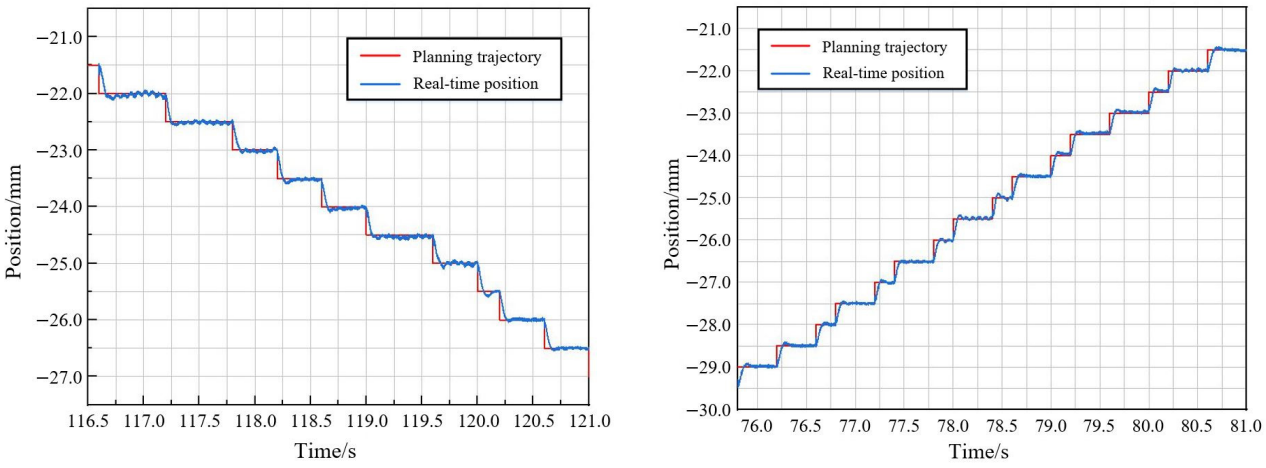


Figure 14. Levitating motion effect during descending motion.

Step-by-step actuation control is engaged in for the position control of the permanent magnet ball to realize large displacement motion and step length is set as 0.5 mm. Figure 15 shows the evolution of the tracking trajectory of the permanent magnet ball that responds to some step inputs with predetermined time intervals. Before every step input, values of controller parameters have been already updated. It can be observed that the large-displacement motion is divided into multi-segment successive small-displacement motion by step-by-step actuation control, and the large-displacement motion of the permanent magnet ball is realized successfully and stably.



(**a**) (**b**)

Figure 15. Levitation motion trajectory of the permanent magnet ball by step-by-step actuation control. (**a**) Descending motion; (**b**) Ascending motion.

6. Conclusions

A neural network PID control of the magnetic levitation actuation and motion control system based on force imbalance is proposed in this paper. In the system, dual electromagnetic actuators are set to generate a superimposed external static magnetic field, and the stable levitation and controllable levitating motion of a permanent magnet ball in a non-liquid environment are realized. Since neural network control has high adaptability to complex systems with nonlinearities and uncertainties, this control method solves the shortcomings that the deviation between the controlled object and the steady-state operating point increases and the tracking performance deteriorates rapidly. Simulations and experiments show that the magnetic levitation actuation and motion control system based on the neural network PID control algorithm is feasible. The neural network PID controller has more stable and accurate dynamic and static performance than the model-based controllers.

Author Contributions: Conceptualization, G.L. and Y.L.; methodology, G.L., Y.L. and J.X.; software, G.L.; validation, G.L., Y.L., J.X. and Z.C.; formal analysis, G.L.; investigation, Z.C. and H.Y.; resources, Y.L. and J.X.; data curation, G.L. and J.X.; writing—original draft preparation, G.L.; visualization, G.L., J.X. and H.Y.; supervision, Y.L. and J.X. All authors have read and agreed to the published version of the manuscript.

Funding: This research was funded by National Natural Science Foundation of China, grant numbers 51975293 (Yonghua Lu) and 52205018 (Jiajun Xu) and Aeronautical Science Foundation of China, grant number 2019ZD052010 (Yonghua Lu).

Institutional Review Board Statement: Not applicable.

Informed Consent Statement: Not applicable.

Data Availability Statement: Not applicable.

Acknowledgments: Authors would also like to appreciate the Test Technology Laboratory of NUAA for providing devices.

Conflicts of Interest: The authors declare no conflict of interest.

References

1. Sun, Z.; Ye, B.; Qiu, Y.; Cheng, X.; Zhang, H.; Liu, S. Preliminary Study of a Legged Capsule Robot Actuated Wirelessly by Magnetic Torque. *IEEE Trans. Magn.* **2014**, *50*, 8105404. [CrossRef]
2. Tang, P.; Liang, L.; Xiang, Y. Measurement and Simulation of Fluid Flow Field in the Pipe of Magnetic Capsule Robot. *Adv. Mech. Eng.* **2020**, *12*, 1687814020985953. [CrossRef]
3. Zhang, Y.; Wang, D.; Guo, D.; Yu, H. Characteristics of Magnetic Torque of a Capsule Micro Robot Applied in Intestine. *IEEE Trans. Magn.* **2009**, *45*, 2128–2135. [CrossRef]
4. Wang, Z.; Yu, Y.; Wang, Q.; Song, T. A Novel Rotating Magnetic Field Generator for Driving Magnetic Micro-machine. *IEEE Trans. Appl. Supercond.* **2008**, *18*, 887–890. [CrossRef]
5. Chi, M.; Zhang, J.; Liu, R.; Wang, Y.; Nie, G.; Qian, X. Coupled Steering Control of a Low Torsional Torque Capsule Robot in the Intestine. *Mechatronics* **2021**, *77*, 102596. [CrossRef]
6. Liu, X.; Mancini, G.J.; Tan, J. Design and Analysis of a Magnetic Actuated Capsule Camera Robot for Single Incision Laparoscopic Surgery. In Proceedings of the 2015 IEEE/RSJ International Conference on Intelligent Robots and Systems (IROS), Hamburg, Germany, 28 September–3 October 2015; pp. 229–235.
7. Kummer, M.P.; Abbott, J.J.; Kratochvil, B.E.; Borer, R.; Sengul, A.; Nelson, B.J. An Electromagnetic System for 5-DOF Wireless Micromanipulation. *IEEE Trans. Robot.* **2010**, *26*, 1006–1017. [CrossRef]
8. Byun, D.; Choi, J.; Cha, K.; Park, J.O.; Park, S. Swimming Microrobot Actuated by Two Pairs of Helmholtz Coils System. *Mechatronics* **2011**, *21*, 357–364. [CrossRef]
9. Jang, G.B.; Jeon, S.; Nam, J.; Lee, W.; Jang, G. A Spiral Microrobot Performing Navigating Linear and Drilling Motions by Magnetic Gradient and Rotating Uniform Magnetic Field for Applications in Unclogging Blocked Human Blood Vessels. *IEEE Trans. Magn.* **2015**, *51*, 9100404. [CrossRef]
10. Ye, B.; Zhang, W.; Sun, Z.J.; Lin, G.; Chao, D.; Chen, Y.Q.; Zhang, H.H.; Sheng, L. Study on a Magnetic Spiral-type Wireless Capsule Endoscope Controlled by Rotational External Permanent Magnet. *J. Magn. Magn. Mater.* **2015**, *395*, 316–323. [CrossRef]
11. Yim, S.; Sitti, M. Design and Rolling Locomotion of a Magnetically Actuated Soft Capsule Endoscope. *IEEE Trans. Robot.* **2012**, *28*, 183–194. [CrossRef]

12. Zhou, H.; Alici, G.; Than, T.D.; Li, W.; Martel, S. Magnetic Propulsion of a Spiral-type Endoscopic Microrobot in a Real Small Intestine. In Proceedings of the 2012 IEEE/ASME International Conference on Advanced Intelligent Mechatronics (AIM), Kaohsiung, China, 11–14 July 2012; pp. 63–68.
13. Ishiyama, K.; Sendoh, M.; Yamazaki, A.; Arai, K.I. Swimming Micro-machine Driven by Magnetic Torque. *Sens. Actuators A Phys.* **2001**, *91*, 141–144. [CrossRef]
14. Dreyfus, R.; Baudry, J.; Roper, M.L.; Fermigier, M.; Stone, H.A.; Bibette, J. Microscopic Artificial Swimmers. *Nature* **2005**, *437*, 862–865. [CrossRef]
15. Marino, H.; Bergeles, C.; Nelson, B.J. Robust Electromagnetic Control of Microrobots Under Force and Localization Uncertainties. *IEEE Trans. Autom. Sci. Eng.* **2013**, *11*, 310–316. [CrossRef]
16. Zhang, J.; Wang, X.; Shao, X. Design and Real-Time Implementation of Takagi–Sugeno Fuzzy Controller for Magnetic Levitation Ball System. *IEEE Access* **2020**, *8*, 38221–38228. [CrossRef]
17. Chen, W.; Meng, X.; Li, J. PID Controller Design of Maglev Ball System Based on Chaos Parameters Optimization. In Proceedings of the 2010 International Conference on Machine Vision and Human-machine Interface, Kaifeng, China, 24–25 April 2010; pp. 772–775. [CrossRef]
18. Zhang, C.; Wu, X.; Xu, J. Particle Swarm Sliding Mode-Fuzzy PID Control Based on Maglev System. *IEEE Access* **2021**, *9*, 96337–96344. [CrossRef]
19. Choi, J.S.; Baek, Y.S. A Single Dof Magnetic Levitation System Using Time Delay Control and Reduced Order Observer. *KSME Int. J.* **2002**, *16*, 1643–1651. [CrossRef]
20. Cho, D.; Kato, Y.; Spilman, D. Sliding Mode and Classical Controllers in Magnetic Levitation Systems. *IEEE Control Syst. Mag.* **1993**, *13*, 42–48. [CrossRef]
21. José, D.J.R.; Zhang, L.; Lughofer, E.; Cruz, P.; Alsaedi, A.; Hayat, T. Modeling and Control with Neural Network for a Magnetic Levitation System. *Neurocomputing* **2017**, *227*, 113–121. [CrossRef]
22. Shao, H. Delay-dependent Stability for Recurrent Neural Network with Time-varying Delays. *IEEE Trans. Neural Netw.* **2008**, *19*, 1647–1651. [CrossRef]
23. Gao, X.; Liao, L. A New One-layer Neural Network for Linear and Quadratic Programming. *IEEE Trans. Neural Netw.* **2010**, *21*, 918–929. [CrossRef]
24. Chu, Y.; Fei, J.; Hou, S. Adaptive Global Sliding-mode Control for Dynamic Systems Using Double Hidden Layer Recurrent Neural Network Structure. *IEEE Trans. Neural Netw. Learn. Syst.* **2020**, *31*, 1297–1309. [CrossRef] [PubMed]
25. Daghooghi, Z.; Menhaj, M.; Zomorodian, A.; Akramizadeh, A. A Real-time Control of Maglev System Using Neural Network and Genetic Algorithms. In Proceedings of the 2012 IEEE International Conference on Industrial Technology, Athens, Greece, 19–21 March 2012; pp. 527–532.
26. Hanh, D.L.; Ahn, K.K.; Kha, N.B.; Jo, W.K. Trajectory Control of Electro-hydraulic Excavator Using fuzzy Self Tuning Algorithm with Neural Network. *J. Mech. Sci. Technol.* **2009**, *23*, 149–160. [CrossRef]
27. Liu, Q.; Xu, X.; Chen, Y. Study on PID Neural Network Decoupling Control of Pneumatic Membrane Structure Inflation System. In Proceedings of the 2011 International Symposium on Information and Automation (ISIA), Berlin/Heidelberg, Germany, 10–11 November 2010; pp. 704–710.

Disclaimer/Publisher's Note: The statements, opinions and data contained in all publications are solely those of the individual author(s) and contributor(s) and not of MDPI and/or the editor(s). MDPI and/or the editor(s) disclaim responsibility for any injury to people or property resulting from any ideas, methods, instructions or products referred to in the content.